INTERNATIONAL JOURNAL FOR NUMERICAL METHODS IN FLUIDS, VOL. 2, 253–261 (1982)

NUMERICAL INTEGRATION OF THE SHALLOW WATER EQUATIONS OVER A SLOPING SHELF

B. JOHNS

Department of Meteorology, University of Reading, U.K.

SUMMARY

A finite-difference method is described for the numerical integration of the one-dimensional shallow water equations over a sloping shelf that allows for a continuously moving shoreline. An application of the technique is made to the propagation of non-breaking waves towards the shoreline. The results of the computation are compared with an evaluation based upon an exact analytical treatment of the non-linear equations. Excellent agreement is found for both tsunami and tidal scale oscillations.

KEY WORDS Shallow Water Equations Sloping Shelf Moving Shoreline Finite-difference Integration

1. INTRODUCTION

Models of fluid systems based on the shallow water equations are widely used in oceanography. In the coastal environment, there exist well-documented studies of tides, surges, tsunami propagation and wave run-up on beaches. One particular problem often faced by the numerical modeller in this area is that of treating a moving shoreline. Various *ad hoc* methods have been used by different investigators. Among these, we may mention Flather and Heaps[1] in an investigation of tides, and Johns[2] and Johns and Jefferson[3] in a study of surface wave propagation through the surf zone. On the tidal scale, the usual practice has been to allow the shoreline to advance discontinuously from one grid-point to the next subject to some suitable criterion. The procedure used by the present author in the surf zone calculations depends on the shoreline displacement being limited to about one grid-increment in the finite-difference discretization of the problem. Clearly, this may impose a severe restriction on the application of the method.

Other numerical treatments of the moving shoreline problem have been given by Sielecki and Wurtele,[4] who pioneered a method of integrating the shallow water equations with sloping boundaries. In a storm surge context, Reid and Bodine[5] have also described a finite-difference method of treating a moving shoreline which is advanced discontinuously from one fixed grid point to the next. Jamet and Bonnerot[6] have given a finite element method in both space and time which incorporates a continuously deforming spatial grid. Lynch and Gray[7] have described a finite element method for flow in a deforming region governed by the shallow water equations. This latter method is particularly attractive because it allows for the continuous movement of the shoreline.

In the present paper, we describe a simple finite-difference procedure that admits the treatment of a continuously moving shoreline. The method is a development of a scheme originally used by Johns *et al.*[8] for representing a fixed curvilinear boundary in a storm surge model; this was subsequently generalized by Johns *et al.*[9] to the case of a moving shoreline.

0271–2091/82/030253–09$01.00

Received 24 August 1981
Revised 19 November 1981

The purpose here is to demonstrate the efficacy of the method by simulating standing waves over a sloping shelf and comparing the numerical solution with the evaluation of an exact analytical solution given by Carrier and Greenspan.[10] We consider examples relevant to both tsunami and tidal scales. In each of these, agreement between the numerical and exact solutions is found to be satisfactory to within about 4 per cent.

2. FORMULATION

Rectangular Cartesian axes are used in which the x-axis is directed landward from a point, O, situated in the undisturbed level of the free surface. Oz points vertically upwards. The equilibrium length of the analysis region is L and there is a sloping shelf above which the equilibrium depth decreases linearly from h_0 at O to zero at the undisturbed position of the shoreline. The disturbed position of the free surface is at $z = \zeta(x, t)$. The usual shallow water equations satisfied by ζ and the velocity, u, may then be written

$$\frac{\partial \zeta}{\partial t}+\frac{\partial}{\partial x}[(\zeta+1-x)u]=0 \tag{1}$$

$$\frac{\partial u}{\partial t}+u\frac{\partial u}{\partial x}+\frac{\partial \zeta}{\partial x}=0. \tag{2}$$

In (1) and(2), the horizontal distance is scaled by L, the time by $L/(gh_0)^{1/2}$, the velocity by $(gh_0)^{1/2}$, and the elevation by h_0.

With this scaling, the elevation is prescribed at $x=0$ in the form

$$\zeta = \varepsilon \cos\left(\frac{2\pi t}{T}\right), \tag{3}$$

where the scaled wave period, T, is related to the dimensional period, T_p, by

$$T=\frac{(gh_0)^{1/2}T_p}{L}. \tag{4}$$

The scaled wave amplitude, ε, is related to the dimensional amplitude, a, by

$$\varepsilon = \frac{a}{h_0}. \tag{5}$$

As the waves propagate towards the shoreline, we stipulate that the instantaneous position of the shoreline corresponds to

$$x = 1+\xi(t), \tag{6}$$

where ξ represents the scaled inland displacement of the shoreline from its equilibrium position. The boundary conditions at the shoreline are the kinematical condition:

$$u=\frac{d\xi}{dt} \quad \text{at} \quad x=1+\xi \tag{7}$$

and a statement of zero water depth:

$$\xi=\zeta \quad \text{at} \quad x=1+\xi. \tag{8}$$

As shown by Carrier and Greenspan[10] these equations may, in certain circumstances, admit of an oscillatory solution representating a non-breaking standing wave in which the shoreline moves up and down the sloping shelf. With the present notation, it is easy to show that

$$\zeta = -\tfrac{1}{2}u^2 + AJ_0\left(\frac{4\pi\alpha}{T}\right)\cos\left(\frac{2\pi\beta}{T}\right) \tag{9}$$

$$u = -\frac{4AJ_1\left(\frac{4\pi\alpha}{T}\right)}{\alpha}\sin\left(\frac{2\pi\beta}{T}\right), \tag{10}$$

where

$$\left.\begin{aligned}\alpha &= (1+\zeta-x)^{1/2}\\ \beta &= t+u\end{aligned}\right\}, \tag{11}$$

and J_0 and J_1 denote Bessel functions of the first kind.

The displacement of the shoreline may be deduced from

$$\xi = \left[-\tfrac{1}{2}u^2 + A\cos\left(\frac{2\pi\beta}{T}\right)\right]_{\alpha=0}. \tag{12}$$

The amplitude factor, A, may be fixed in terms of ε by linearizing (9) at $x=0$ and matching the resultant with (3). This yields

$$A = \frac{\varepsilon}{J_0\left(\frac{4\pi}{T}\right)}. \tag{13}$$

It should be noted that the linearization of (9) at $x=0$ is not necessarily an essential part of the solution process but is consistent with our subsequent linearization of (2) at $x=0$. In the numerical procedure, if the spatial variation of u at $x=0$ is unknown, the linearization of (2) at $x=0$ will always be necessary and it must therefore be a valid approximation. In the example considered here, the non-linear variation of both ζ and u with x and t could in fact be computed to any degree of accuracy by use of (9) and (10) and, in consequence, the linearization procedure at $x=0$ is not strictly necessary. In more general circumstances where an analytical solution does not exist, this option is not available and the application of the method depends upon the solution for ζ and u at $x=0$ being effectively determined by linear equations. In the examples considered later, the variation of ζ implied by (9) is indeed effectively linear at $x=0$ and, on approaching $x=1+\xi$, it becomes increasingly distorted by non-linearity as described by Carrier and Greenspan.[10] One reason for our method of treatment is that it enables us to describe the application of the technique in situations where the exact form of spatial and temporal variation of both ζ and u at $x=0$ is unknown and where the sole input information is that both ζ and u have a sinusoidal variation with t corresponding to that given in (3). A second reason is because of the considerably simplified form of the input conditions, and the ease of application, that results from the linearization process.

In Section 3, we give a numerical method of treating (1), (2), (7) and (8) and subsequently describe experiments in which the numerical solution is compared with an evaluation of the implicitly defined analytical solution.

3. NUMERICAL TECHNIQUE

We define a new variable, X, by

$$X = \frac{x}{1+\xi}, \tag{14}$$

so that the shoreline always corresponds to $X=1$. With X and t as new independent variables, (1) and (2) may be transformed to

$$\frac{\partial F}{\partial t} + \frac{1}{1+\xi}\frac{\partial}{\partial X}(UF) = 0 \tag{15}$$

and

$$\frac{\partial G}{\partial t} + \frac{1}{1+\xi}\frac{\partial}{\partial X}(UG) + \frac{F}{1+\xi}\frac{\partial \zeta}{\partial X} = 0 \tag{16}$$

where

$$\left.\begin{aligned} F &= (1+\xi)H \\ G &= (1+\xi)Hu \end{aligned}\right\} \tag{17}$$

$$H = 1 + \zeta - (1+\xi)X \tag{18}$$

and

$$U = u - X\frac{d\xi}{dt}. \tag{19}$$

When $X=1$,

$$U = (u)_{x=1+\xi} - \frac{d\xi}{dt}. \tag{20}$$

Hence, (7) is satisfied by ensuring that

$$U = 0 \quad \text{at} \quad X = 1. \tag{21}$$

Our approach will be to generate an oscillatory solution of (15) and (16) by integrating ahead in time from an initial state of rest with an off-shore forcing corresponding to (3). We therefore define a discrete sequence of grid-points in the X-space given by

$$X = X_i = (i-1)\,\Delta X; \qquad i = 1, 2, \ldots m; \qquad \Delta X = 1/(m-1) \tag{22}$$

and a discrete sequence of time instants by

$$t = t_p = p\,\Delta t; \qquad p = 0, 1, \ldots . \tag{23}$$

For any variable, χ, we write

$$\chi(X_i, t_p) = \chi_i^p. \tag{24}$$

The grid-points are staggered and are of two distinct types. When i is odd, we refer to the point as a ζ-point at which F and ζ are computed. When i is even, the point is a u-point at which G, u and U are computed. Therefore, m must be even and then corresponds to a point at which $U \equiv 0$ thus satisfying (21).

To facilitate the description of the finite-difference equations, we define difference operators by

$$\left.\begin{aligned}\Delta_t\chi &= (\chi_i^{p+1}-\chi_i^p)/\Delta t\\ \delta_X\chi &= (\chi_{i+1}^p-\chi_{i-1}^p)/(2\Delta X)\end{aligned}\right\}. \quad (25)$$

An averaging operation is defined by

$$\bar{\chi}^X = \tfrac{1}{2}(\chi_{i+1}^p+\chi_{i-1}^p) \quad (26)$$

and a shift operator by

$$E_t\chi = \chi_i^{p+1}. \quad (27)$$

Discretizations of (15) and (16) are based upon a scheme given by Sielecki[11] and are derived from

$$\Delta_t F + \frac{1}{1+\xi}\,\delta_X(U\bar{F}^X) = 0 \quad (28)$$

and

$$\Delta_t G + \frac{1}{1+\xi}\,\delta_X(\bar{U}^X\bar{G}^X) + E_t\left[\frac{\bar{F}^X}{1+\xi}\,\delta_X\zeta\right] = 0. \quad (29)$$

Equation (28) leads to an updating procedure for F at the interior ζ-points. ζ may then be deduced by applying

$$\zeta = -1+(1+\xi)X+\frac{F}{1+\xi}. \quad (30)$$

This procedure does not, however, yield the updated value of ζ at $X=0$ which must be determined through use of (3). Writing

$$\mu(x,t) = u+2(1+\zeta-x)^{1/2}, \quad (31)$$

the theory of characteristics discussed by Stoker[12] shows that μ must be prescribed as a function of t at some position x. In the present work, we linearize (31) and prescribe μ at $x=(1+\xi)\Delta X$ evaluating the known solution for ζ and u at this position by a corresponding linearization of (9) and (10). This procedure then yields

$$\theta u_2^p + \zeta_2^{p+1} = A\left[J_0\left(\frac{4\pi\theta}{T}\right)\cos(\tau) - J_1\left(\frac{4\pi\theta}{T}\right)\sin(\tau)\right] \quad (32)$$

where

$$\theta = [1-(1+\xi^p)\,\Delta X]^{1/2} \quad (33)$$

and

$$\tau = \frac{2\pi t_{p+1}}{T}. \quad (34)$$

Again, this linearization is not essential in the present application since the non-linear variation of $\mu(x,t)$ at $x=(1+\xi)\,\Delta X$ could be determined as a function of t by use of (9), (10) and (11). From this variation, (31) could then be used to compute ζ_2^{p+1} in terms of u_2^p with the incorporation of the full non-linearity. As stated earlier, however, the effect of this non-linearity is negligible near $x=0$ and its inclusion serves no purpose other than to complicate the input conditions. Moreover, in more general applications, this option is not available since the exact form of both ζ and u is unknown. In these circumstances, our linearization technique permits a straightforward application to be made when $\theta\, u_2^p + \zeta_2^{p+1}$ has a prescribed sinusoidal variation with t.

It will be noted that u and ξ are evaluated at the lower time level at which they are already known. However, ζ and τ are evaluated at the advanced time level. This, of course, introduces a truncation error $O(\Delta t)$ into the numerical solution. The elevation is not computed at $i=2$ and so we use

$$\zeta_2^{p+1} = \tfrac{1}{2}(\zeta_1^{p+1} + \zeta_3^{p+1}). \tag{35}$$

When (35) is combined with (32) it is possible to update ζ at $X=0$ in a way that is consistent with (3) and the known linearized form of the solution at the seaward end of the analysis region.

The correspondingly updated value of ξ is then inferred by using (8) and is simply equal to ζ_m^{p+1}. However, since ζ is not carried at $i=m$ its value there is determined by linear extrapolation from adjacent ζ-points. This leads to

$$\zeta_m^{p+1} = \tfrac{1}{2}(3\,\zeta_{m-1}^{p+1} - \zeta_{m-3}^{p+1}). \tag{36}$$

These updated values of ζ may then be used in (16) to update G at the u-points. When (16) is applied at $i=2$, the non-linear advective term is omitted; this is consistent with the linearized form of the boundary condition (32). The updated values of u are found from

$$u = \frac{G}{\bar{F}^X}. \tag{37}$$

Finally, before proceeding to the next updating cycle, the updated value of U must be deduced at the u-points. This is readily determined in terms of known quantities using a discrete version of (19) based upon

$$E_t U = E_t u - X\,\Delta_t \xi. \tag{38}$$

4. NUMERICAL EXPERIMENTS

We take $\varepsilon = 1/500$ and $T = 1{\cdot}26$. This parameter setting is chosen so that corresponding dimensional quantities are $L = 50$ km, $h_0 = 500$ m, $T_p = 15$ mins and $a = 1{\cdot}0$ m. Thus, we consider a tsunami scale of oscillation over a steeply sloping continental shelf. The finite-difference scheme is applied with $m = 100$ and $\Delta t = T/360$. It is found that the response is essentially oscillatory after 4 complete cycles of integration—thus demonstrating the effectiveness of (32) in allowing the initial transient response to be radiated across the seaward boundary and out of the analysis region. A diagnostic study is made of the 5th cycle of integration. In Figure 1, we give the spatial variation of ζ at $t=0$ and $t=T/2$, the time origin now referring to the commencement of the 5th cycle. The numerically computed variation is indistinguishable from the exact variation of ζ as calculated by an iterative procedure applied to (9), (10) and (11). As might be expected, the maximum difference occurs in the extrapolated values of ζ at the shoreline. At $t=0$, the computed and exact dimensional values in metres are respectively $-3{\cdot}92$ and $-4{\cdot}09$ whereas at $t=T/2$ they are $4{\cdot}02$ and $4{\cdot}09$ thus indicating errors of approximately 4 and 2 per cent. The accuracy of the numerical

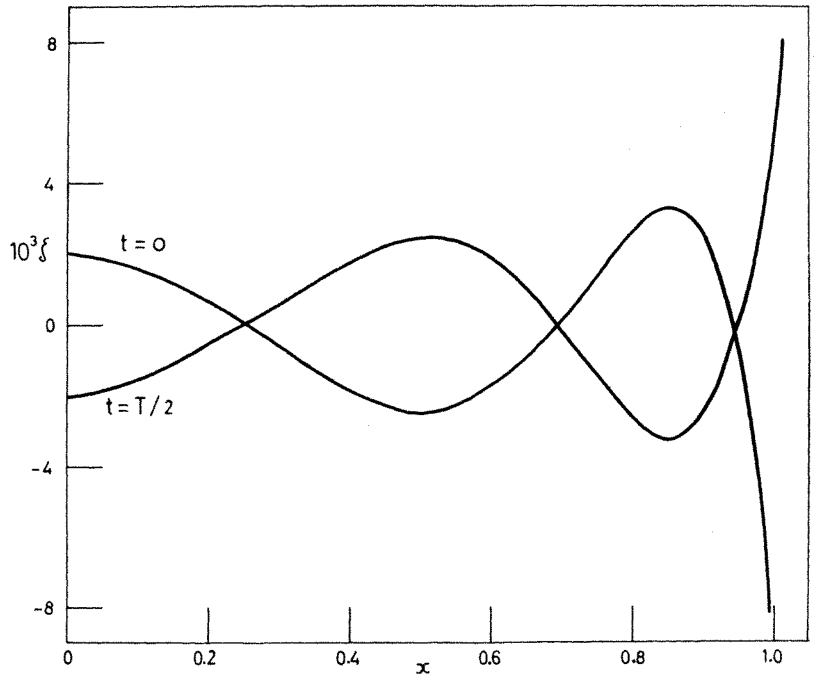

Figure 1. Numerically computed spatial variation of ζ at $t = 0$ and $t = T/2$ with $\varepsilon = 1/500$ and $T = 1{\cdot}26$

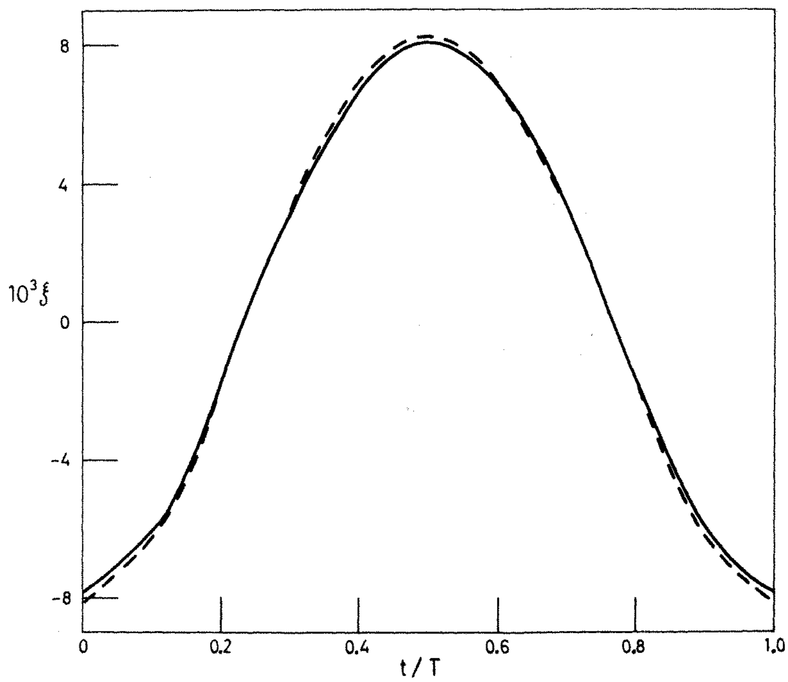

Figure 2. Variation of shoreline displacement during a wave cycle with $\varepsilon = 1/500$ and $T = 1{\cdot}26$
———— Numerical solution
------ Exact solution

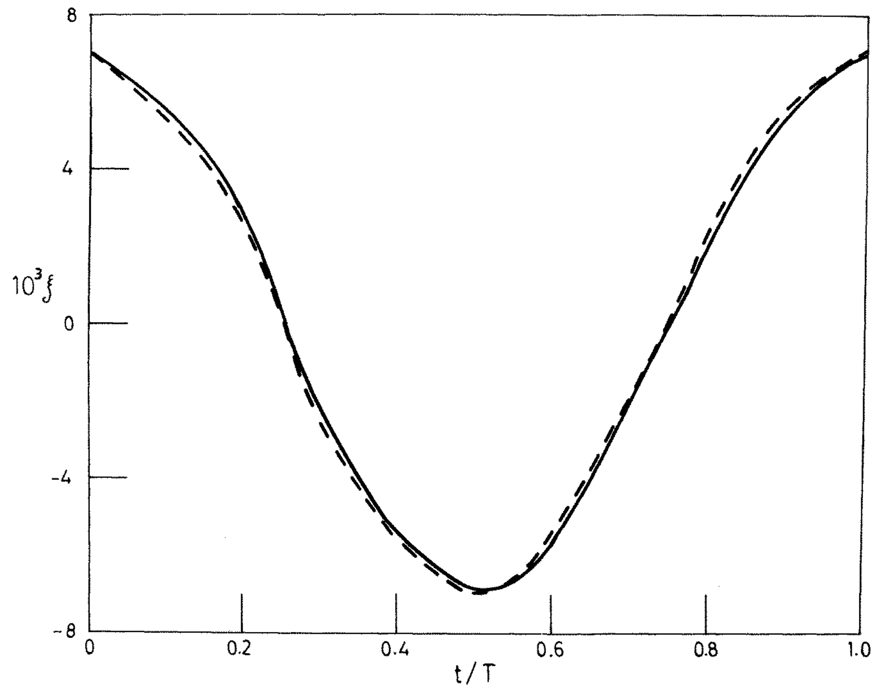

Figure 3. As Figure 2 except that $\varepsilon = 1/300$ and $T = 8{\cdot}07$

solution throughout the wave cycle is most readily appraised by considering the time history of the shoreline displacement. This is given in Figure 2 together with an exact evaluation of ξ determined from (12). From this, we note that the numerical solution underestimates both the maximum shoreline recession and the maximum shoreline intrusion. The percentage errors are, of course, equivalent to those given for the shoreline elevation.

In a second example, we take $\varepsilon = 1/300$ and $T = 8{\cdot}07$. A dimensional equivalent of this setting is $L = 300$ km, $h_0 = 300$ m, $T_p = 12{\cdot}4$ hrs and $a = 1{\cdot}0$ m. This therefore corresponds to a tidal scale of oscillation in which the wavelength is many times greater than the shelf width. In the numerical procedure, we take $m = 50$ and $\Delta t = T/496$ and, as before, obtain an oscillatory response after 4 cycles of integration. The interval $0 \leqslant x \leqslant 1 + \xi$ now accommodates only a fraction of a complete wavelength. Accordingly, a plot of the surface elevation will not show the same prominent wave-like characteristics as in the case of tsunamis. In fact, the computed and exact values of ζ never differ by more than 2 per cent but the effectiveness of the numerical scheme is best demonstrated by considering the temporal variation of the shoreline displacement. This is the most sensitive indicator of any discrepancy between the numerical and exact solution and is given in Figure 3 together with exact evaluation of ξ determined from (12). It is clear that agreement between the computed and exact value of the shoreline displacement is good with regard to both amplitude and phase.

Our conclusion is that the numerical method described in this paper is an effective way of treating the moving shoreline problem for the parameter settings considered. The work complements that given by Johns *et al.*[8] where a two-dimensional version of the method is applied in a storm surge context. In that study, an exact analytical solution does not exist for comparison and it is our submission that the present work provides support for the methods used in the more general case.

REFERENCES

1. R. A. Flather and N. S. Heaps, 'Tidal computations for Morecambe Bay', *Geophys. J. R. Astr. Soc.*, **42,** 489–517 (1975).
2. B. Johns, 'The modelling of the approach of bores to a shoreline', *Coastal Eng.*, **3,** 207–219 (1980).
3. B. Johns and R. J. Jefferson, 'The numerical modelling of surface wave propagation in the surf zone,' *J. Phys. Oceanogr.*, **10,** 1061–1069 (1980).
4. A. Sielecki and M. G. Wurtele, 'The numerical integration of the non-linear shallow water equations with sloping boundries', *J. Comp. Phys.*, **6,** 219–236 (1970).
5. R. O. Reid and B. R. Bodine, 'Numerical model for storm surges in Galveston Bay', *Proc. Am. Soc. Civ. Eng., J. Waterways Harbours Div.*, **94,** 33–57 (1968).
6. P. Jamet and R. Bonnerot, 'Numerical solution of the Eulerian equations of compressible flow by finite element method which follows the free boundary and the interfaces', *J. Comp. Phys.*, **18,** 21–45 (1975).
7. D. R. Lynch and W. G. Gray, 'Finite element simulation of flow in deforming regions', *J. Comp. Phys.*, **36,** 135–153 (1980).
8. B. Johns, S. K. Dube, U. C. Mohanty and P.C. Sinha, 'Numerical simulation of the surge generated by the 1977 Andhra cyclone', *Quart. J. R. Met. Soc.*, **107,** 919–934 (1981).
9. B. Johns, S. K. Dube, P. C. Sinha, U. C. Mohanty and A. D. Rao, 'The simulation of a continuously deforming lateral boundary in problems involving the shallow water equations', *Computers and Fluids*, (in press, 1982).
10. G. F. Carrier and H. P. Greenspan, 'Water waves of finite amplitude on a sloping beach', *J. Fluid Mech.*, **4,** 97–109 (1958).
11. A. Sielecki, 'An energy-conserving difference scheme for the storm surge equations', *Mon. Wea. Rev.*, **96,** 150-156 (1968).
12. J. J. Stoker, *Water waves*, Interscience, New York, 1957.